THE PENNSYLVANIA STATE UNIVERSITY
SCHREYER HONORS COLLEGE

DEPARTMENT OF PHYSICS

DYNAMIC BUCKLING OF FREE RODS IN FLIGHT

STEVEN J. FULL
Spring 2010

A thesis
submitted in partial fulfillment
of the requirements
for a baccalaureate degree
in Physics
with honors in Physics

Reviewed and approved by the following

Andrew Belmonte
Associate Professor
Thesis Supervisor

Richard Robinett
Associate Department Head
Honors Adviser

*Signatures are on file in the Schreyer Honors College.

Abstract

In this thesis we present a study of the buckling of free rods both in flight and undergoing accelerations, specifically in the context of a bow and arrow system. In archery, the phenomenon of an arrow flexing around the bow is more commonly known as Archer's Paradox, and is a problem of extreme significance to archers.

We study the buckling of an arrow experimentally by capturing and analyzing high speed videos and attempt to model the phenomena mathematically. From the high speed videos we are able to track the position of the nock and tip of the arrow as a function of time and use it to indirectly obtain the compression forces and fictitious forces experienced by an accelerating arrow in its non-inertial rest frame. These forces can eventually be used to solve the equations which govern the buckling of an arrow as it is being accelerated. In addition, several images of the buckling of an arrow were obtained which can validate such a mathematical model.

The dynamic Euler-Bernoulli buckling equation is modified to model the buckling of an arrow both in flight and as it is being accelerated. The general strategy is model the buckling of the arrow as vibrations about its center of mass in its rest frame. In order to proceed with such a solution the dynamic Euler-Bernoulli buckling equation is derived for a non-inertial reference frame. It is found that the fictitious force acting on the arrow in the rest frame has major consequences on the vibration of the arrow.

Contents

Acknowledgements

I would like to thank Andrew Belmonte, Robert Geist and my father, James Full, for all of the help they provided me throughout the course of this project.

Chapter 1

Archery and Archer's Paradox

1.1 Introduction and Motivation

Archer's Paradox is historically central to the development of archery throughout the ages. Traditional archers, particularly those who used longbows, designed their bow in such a way that, when released, an arrow must buckle and flex around the handle [2, 4]. In the context of this paper, we define buckling to be the vibrations perpendicular to the direction of travel for the arrow. Their reason for doing this was very simple. A longbow accelerates an arrow outside of the plane of the bow, as illustrated by figure 1. A traditional, instinctive archer will naturally aim down his line of sight and expect his arrow to hit exactly where he was aiming. However, the arrow's trajectory depends entirely on how much it buckles. A stiff arrow will not buckle and, instead of flexing around the handle, will travel in a straight line trajectory landing far to the left of the intended target. Conversely, an arrow which buckles too much will snake around the handle too far and land far to the right of the target. Thus, in order to achieve accuracy, an arrow needs to buckle just the right amount. This phenomenon is known as Archer's Paradox, and is the main motivation for studying the buckling of arrows in flight.

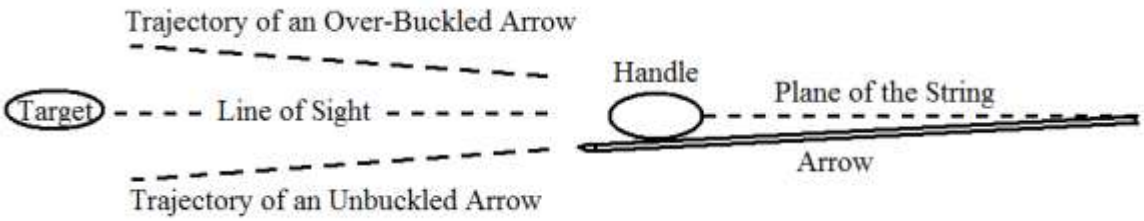

FIG. 1. A top down schematic depicting the cross section of a traditional longbow as it would be held by a right handed archer.

Since the buckling of an arrow outright determines the accuracy of traditional longbow archers, arrow design was historically a topic of great importance. Through experience, longbow archers learned to manipulate the length, diameter and tip weight of their arrows to achieve the desired amount of buckling for maximal accuracy. However, most archers knew very little about the physics of buckling and instead relied on trial and error to find the perfect arrow for their bow. This process of trial and error is commonly called tuning an arrow to a bow, and it remains the dominant practice even today. The only modern advancement on this process is that popular arrow companies, such as Easton, issue fitting charts to aid the consumer in finding arrows that will fit their bow.

Indeed, despite advanced in modern engineering and mathematics, a rather limited number of attempts have been made to model the buckling of an arrow [1-4]. This could be mostly in part due to a lack of motivation. When traditional longbows were replaced with modern center-shot bows, which shoot every arrow down the line of sight, the problem of the buckling of arrows became irrelevant to archers. Even today, the problem still only remains of importance to modern archers who use traditional equipment and competitive shooters who wish to maximize their accuracy to an extreme degree, a small fraction of the archery community.

However, to a curious academic, archer's paradox opens up the window to a new regime of interesting dynamic buckling phenomena. Indeed, a bow and arrow system provides a playground of interesting dynamics and mathematics which could keep a scientist busy for a lifetime. In this thesis I begin exploring the problem both experimentally and theoretically. I use a shooting machine and modern center-shot compound bow to fire arrows and image them using a high speed camera. Then I develop a mathematical equation to describe the vibrations of the arrow as it is being accelerated, and examine some solutions to it.

However, before launching into a direct discussion of the experiment and the mathematical modeling, I present a brief overview of the basic equipment of archery which may be useful to those who are unfamiliar with the sport.

1.2 The Bow

1.2.1 Anatomy of a Bow

The bow is a primitive weapon that has evolved throughout the centuries into its more impressive, modern day form. However, the anatomy of a bow remains largely the same. Bows are comprised of three main parts: the limbs, which store energy, the string, which transfers the energy to the arrow, and the grip or riser, which holds the limbs together. Modern bows also possess a rest just above the grip, which guides the arrow as it is being accelerated. The amount of force that is required to pull back a bow is called the draw weight, and the distance from the grip to the hand of the archer at full draw is called the draw length. The distance between the string and grip when the bow is relaxed

is called the fistmele or braceheight, and is a major factor in the consistency of the bow if it is taken apart and reconstructed.

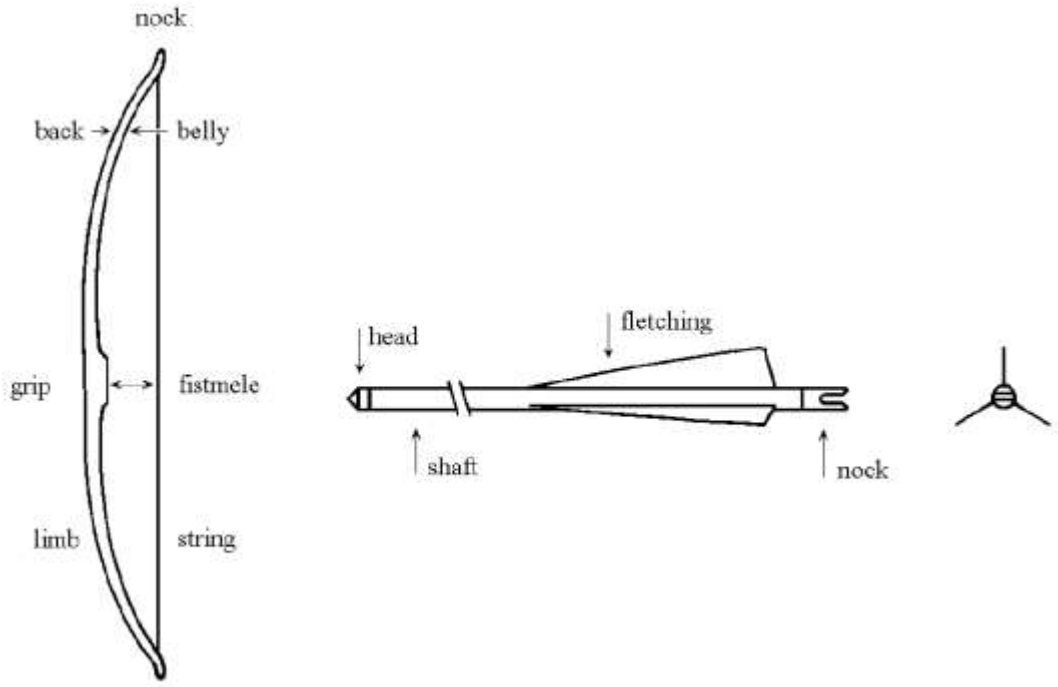

FIG. 2. The anatomy of a longbow and arrow, as drawn by Kooi [2].

1.2.2 Types of Bows

From a modern perspective, all bows can be classified into three main categories: longbows, recurves, and compounds. Longbows are traditional bows known for their accuracy and their large size, typically spanning over 6 feet long. They possess long, straight limbs and are usually made from a single wood stave, although modern variants are constructed out of two pieces which can be detached at the handle for ease of transportation and storage. Instead of using an arrow rest, the archer rests the arrow across his fingers while gripping the bow. Common, everyday depictions of bows are typically that of the longbow, making it the most recognizable of the three types of bows.

A recurve is the closest thing you can get to a traditional bow while still enjoying the perks of modern day engineering. It's most distinctive features are its limbs, which curve backwards away from the archer even when strung. Unlike a longbow, the recurve is a center-shot bow and possesses a rest for the arrow to slide along while being shot. Recurves are also typically designed so that their limbs can be detached from the central grip, called the riser, for the convenience of the archer.

Compounds are undoubtedly the most technically advanced and accurate bows available today. Rather than storing energy solely in the limbs, compounds rely on circular disks called cams to store energy. Their primary function, however, is to reduce the weight of the bow when it is held at full draw. This is called let-off, and it typically decreases the amount of force required to hold the bow in a fully drawn position by 70 to 90 percent, allowing the archer to easily aim the bow for as long as he desires. In addition, modern compounds are typically outfitted with sights and, for long distance shooting, lenses to give the archer pinpoint accuracy. Unlike traditional bows which are made from wood, compounds are typically made from composite materials which give them superior strength and durability. Ultimately, compounds are, hands down, the deadliest and most accurate bows ever created.

1.3 The Arrow

1.3.1 The Anatomy of an Arrow

An arrow is comprised of four main parts, as depicted in figure 2: the shaft, the nock, the head or tip, and the fletching. The shaft is the most important aspect of the arrow in our case, as it determines the main properties of the buckling. Shafts are made

from wood, aluminum, or carbon fiber and, except for some wooden arrows, are hollow in the center to reduce their weight. They come in a wide variety of weights, lengths, diameters, and wall thicknesses to cater for the needs of different types of bows. In our experiments the density of the shaft, its diameter and its wall thickness will play a role in the buckling of the arrow.

The tip of the arrow is the second most important part of the arrow to consider. A wide variety of tips exist from the field tip, designed for target practice, to the deadly broad head, meant for killing game. For this experiment we focus solely on field tips, which come in a variety of different weights but are otherwise essentially identical. A typical field tip weighs 75 to 125 grains (the preferred unit of mass in archery). Tips as heavy as 300 grains are also mass produced but rarely used by the average archer. In this experiment we increase the weight of the tip to increase the magnitude of the buckling of the arrow.

The nock and fletching are the least important aspects of the arrow to consider in the context of buckling. The nock serves only one function: to clamp around the string and keep the arrow in contact with the string as it is pulled back. The perfect nock must be tight enough to clamp snuggly to the string, but loose enough so that, when launched, the arrow smoothly leaves the string. Other than that, the nock is the bland bread and butter of the arrow; there is not much variety to choose from. A Nock typically weighs around 10 grains, making it significantly lighter than the tip of the arrow.

In terms of accuracy, the fletching is hands down the most important part of the arrow. The fletching acts as a stabilizer, correcting any deviations and vibrations of the arrow in flight. Because it works against the motions we are trying to study, we neglect

the effects of the fletching completely by considering and shooting only un-fletched arrows.

Chapter 2

Experimental Apparatus and Techniques

2.1 Methods

A high speed Phantom video camera was used to observe the buckling of arrows in flight and as they were accelerated by a bow. In order to make the firing of the arrows as consistent as possible, we designed and built a modular shooting machine to hold and fire the bow in a very precise way. Unlike many other studies of archer's paradox [1-4], we want to neglect the effects of the shooter's hand and the bow riser on the buckling of the arrow. Thus, in place of a longbow we use a modern center shot 70 lb compound bow with a mechanical release to launch the arrow. The strategy is to use the overwhelming power of a modern bow to buckle the arrow rather than small initial displacements. A system of mirrors allowed us to observe the phenomena from many different angles, making our experimental apparatus very versatile.

Software which came packaged with the camera was used for image analysis. The software allowed us to easily track the position of the arrow as a function of time, and even possessed the ability to calculate the speed and acceleration of captured images. It output the data into a file which could then be analyzed using Microsoft Excel and math packages such as Mathematica.

2.2 Equipment

Below we present a detailed list of the equipment used in this experiment. Most of the archery equipment was old, previously used equipment which were donated by their owners for the sake of science. The shooting machine, however, was constructed entirely from new parts.

- Phantom v. 5.0 High Speed Camera with Phantom Camera Control software
- Darton Wrangler 70lb compound bow
- Ohio Hoist and Pulley 750lb winch
- Bear Archery Bow scale with a 15 - 90lb range, in 1 lb increments
- Tru Fire Mechanical Reslease
- Easton St Epic 600 carbon arrows, with 28 ¾ inch shafts.
- Solid 5/16 inch diameter cedar arrows with 32 inch shafts
- Assorted Field Tips, of weights 100 gr, 125 gr, 150 gr, 200 gr, 250 gr and 300 gr
- "The Block" compressed foam archery target
- White and Black poster boards for a backdrop
- North Star 250 Watt photography light

2.3 The Shooting Machine

A shooting machine was designed and constructed out of 3” diameter PVC pipe to hold and launch the arrow in a consistent way. The goal was to create a frame that was cheap, durable, modular, and that did not obstruct the view of the phenomena. We also needed a frame that was long enough to house a winch to pull back the bow with. Because the camera requires a clear field of view, we designed a rather large frame, approximately 6 feet long and 6 feet high to accommodate for this need. A design blueprint is depicted below in figure 3, and a photograph of the finished product is shown in figure 4.

FIG. 3. A blueprint, courtesy of Robert Geist, showing the design for the shooting machine’s frame.

FIG. 4. A photograph of the shooting machine used during the experiments.

The final design of the shooting machine differed greatly from the initial conception. The entire top half of the frame, originally designed to hold a mirror, was removed because it was found that it was better to hang the mirror directly from the ceiling of the lab. A winch, bow scale, and mechanical release were hung from the frame using rope, as shown in figure 4. To make sure that the bow was pulled back completely straight, a separate PVC pipe was bolted to the first one to provide a track that was more in line with the bow.

The bow itself was lashed using rope to an iron rod jutting out from the pipe. A vice was originally used to hold the bow because it was thought to increase the precision of the experiment by preventing the bow from moving. However, it was found that the

lack of freedom of movement damaged the bow when shot. The lashing was tight enough to hold the bow upright but loose enough to allow the bow to fall forward as it was shot, mimicking the grip of an actual archer. Ultimately, the lashing allowed for solid experimental precision while preserving the quality of the bow.

The winch was required to pull back the bow because of the large amount of force required to pull it back. As a side benefit, the winch allowed for extreme precision in the draw length of the bow. Rather than measure the draw length for each shot, a bow scale was found to be a much better measure of shot consistency, eliminating the need to take into account fistmele and any possible stretching of the string. Overall, the winch allowed for great consistency; each shot possessed the same draw weight to within ±0.1lbs, a remarkable feat.

Ultimately, the shooting machine served its purpose beautifully. Thanks to the winch it was extremely precise. Overall, the shooting machine was of solid design and an extremely cost effective tool.

Chapter 3

Experimental Results

3.1 Force Measurements

3.1.1 Acceleration Curves

Figures 5 and 6 show the position as a function of time of the nock and tip of an Easton St Epic 600 arrow as it is accelerated by a Darton compound bow. The image processing software packaged with the Phantom high speed camera was used to obtain the curves. Specifically, the collect points function was used to analyze the cine file and track the positions of the nock and tip of an arrow as a function of time. The position measurements possessed an experimental error of $\pm 4 \times 10^{-3}$ m due to uncertainties when calibrating the length scales in the images.

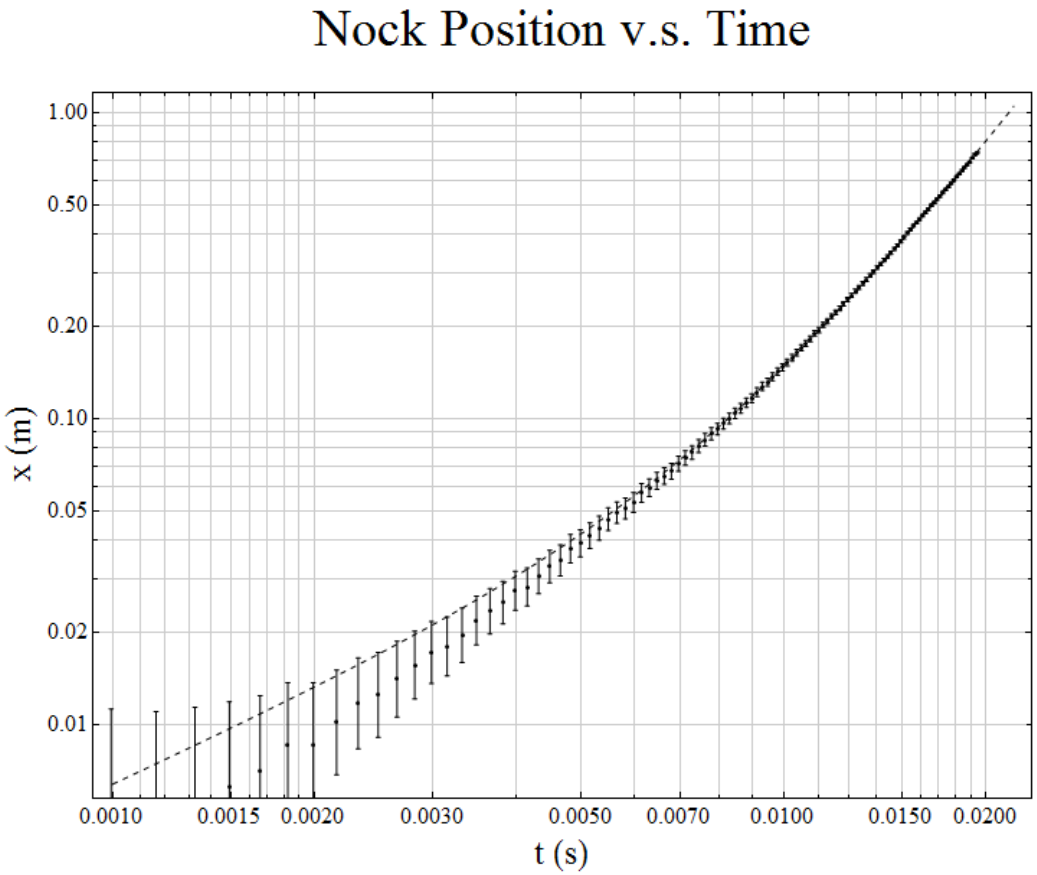

FIG. 5. The position of the nock as a function of time, fit by the dashed curve $x_n(t) = 6.29326\ t + 85059.2\ t^3$.

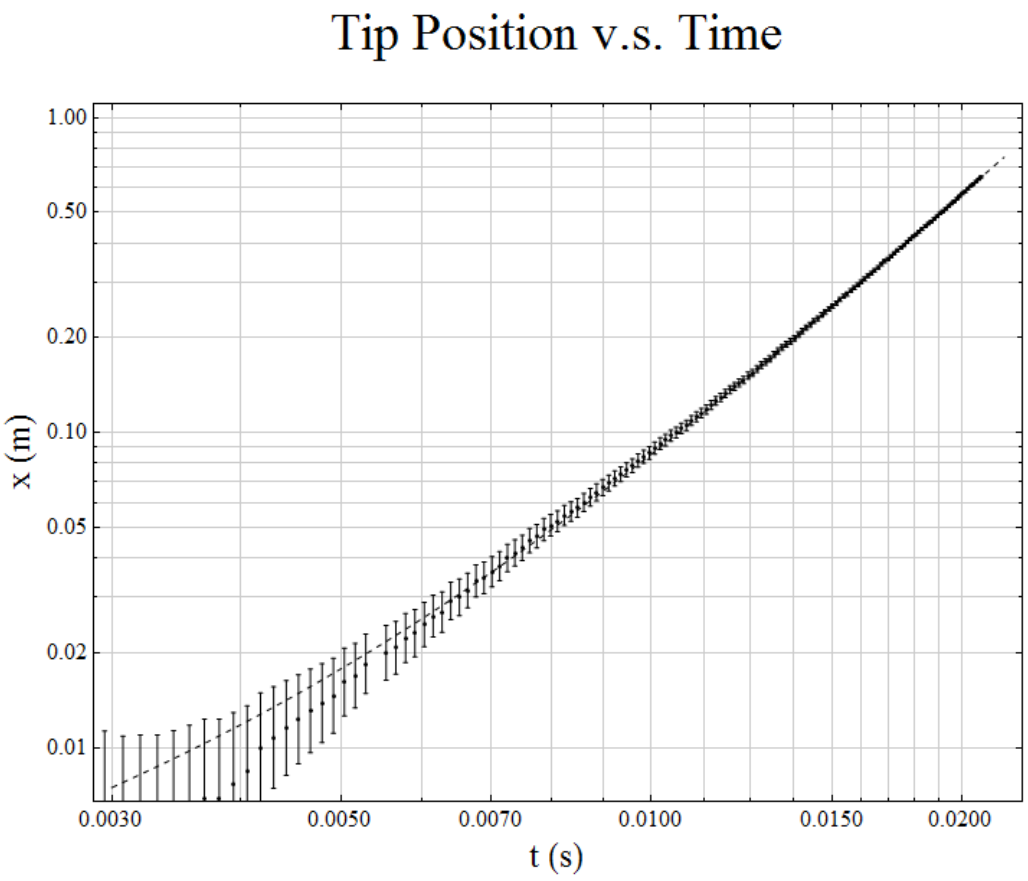

FIG. 6. The position of the nock as a function of time, fit by the dashed curve $x_t(t) = 1.8955\ t + 66437.6\ t^3$.

Once obtained, the data was plotted and a least-squares fit was found by using Mathematica. Through trial and error it was found that the position could be best fit with two free parameters to achieve excellent agreement. The position as a function of time for the nock was found to be $x_n(t) = 6.29326\ t + 85059.2\ t^3$ and the position for the tip was given by $x_t(t) = 1.8955\ t + 66437.6\ t^3$.

3.1.2 Obtaining the Compression and Fictitious Forces

Once the position functions for the tip and nock are found it is a relatively straightforward process to obtain the compression force and fictitious force induced by

solving the equations of vibration in a non-inertial frame. Newton's second law tells us that the force applied to an object is equal to the mass of that object times its acceleration, or F = ma. Acceleration is the second derivative of position with respect to time, or $a(t) = \frac{d^2x(t)}{dt^2}$. So as they are launched, a nock of mass m_n and a tip of mass m_t will experience a force given by F = ma(t).

$$F_t = m_t \frac{d^2x_t(t)}{dt^2} = 6m_t k_t t$$

$$F_n = m_n \frac{d^2x_n(t)}{dt^2} = 6m_n k_n t$$

Where k_n = 85059.2 m/s^3 and k_t = 66437.6 m/s^3 are the experimentally obtained fit parameters.

Now imagine you are the tip of an accelerating arrow. You are accelerating at a rate $6k_t t$ in the lab frame, but in your rest frame you are not accelerating at all. The nock, on the other hand, is accelerating at a rate $6k_n t$ in the lab frame with $k_n > k_t$. A Galilean transformation to the rest frame of the tip tells you that you would observe the nock of the arrow accelerating toward the tip at a rate $6(k_n - k_t)t$. This means that the arrow is being compressed in your frame. Therefore, in this frame the compression force applied to the end of the arrow is simply given by:

$$F_c = 6m_n(k_n - k_t)t$$

The fictitious force, on the other hand, is given by the acceleration experienced by the center of mass of the arrow. When making a change of coordinates to a non-inertial frame, the laws of Physics change slightly so you must take into account a new fictitious force in your equations. For the case of a tip-less arrow with constant density, the fictitious force is equal to the average of the acceleration at the tip and the nock:

$$f = 3m_n(k_n - k_t)t$$

When trying to obtain the fictitious force for an arrow with a tip, the terms must be weighted so that you obtain the acceleration located at the center of mass and not just the acceleration of the center of the arrow.

3.2 High Speed Images

In this section we present some images taken from high speed videos of an arrow in flight which can be used to validate the mathematical model. In figure 7 we present the buckling of an Easton St Epic 600 arrow captured at 2100 fps with an exposure time of 28μs. Figure 8 shows the same exact arrow with a 300 grain tip undergoing extreme buckling captured at 8000 fps with an exposure time of 210μs. Figure 9 shows the buckling of a cedar arrow with a 150 grain tip captured at 2100 fps with an exposure time of 28μs. Higher tip weights resulted in the cedar arrow being shattered as it was accelerated by the bow, an extremely unsafe scenario!

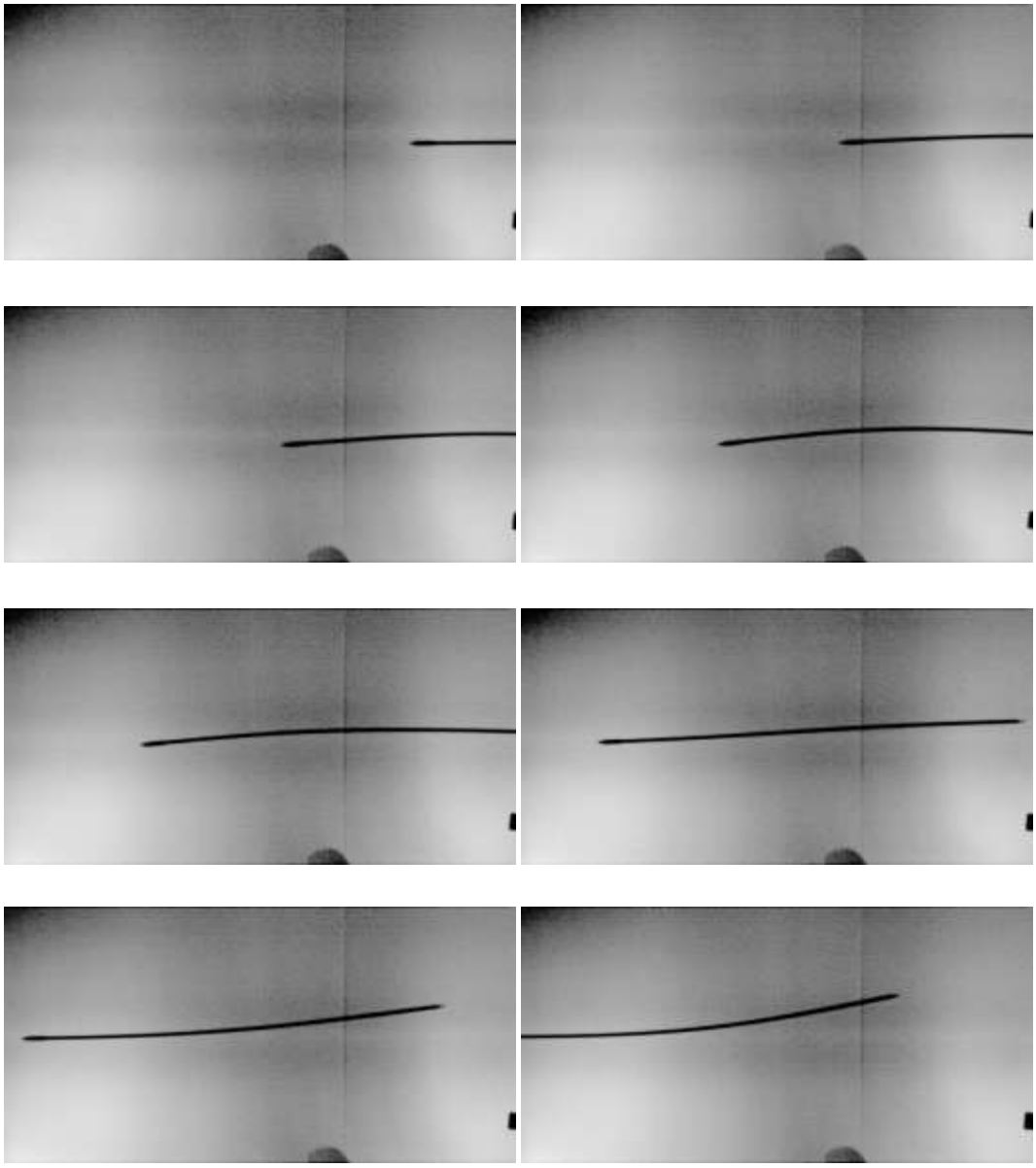

FIG. 7. The buckling of a carbon arrow flying from the right to the left.

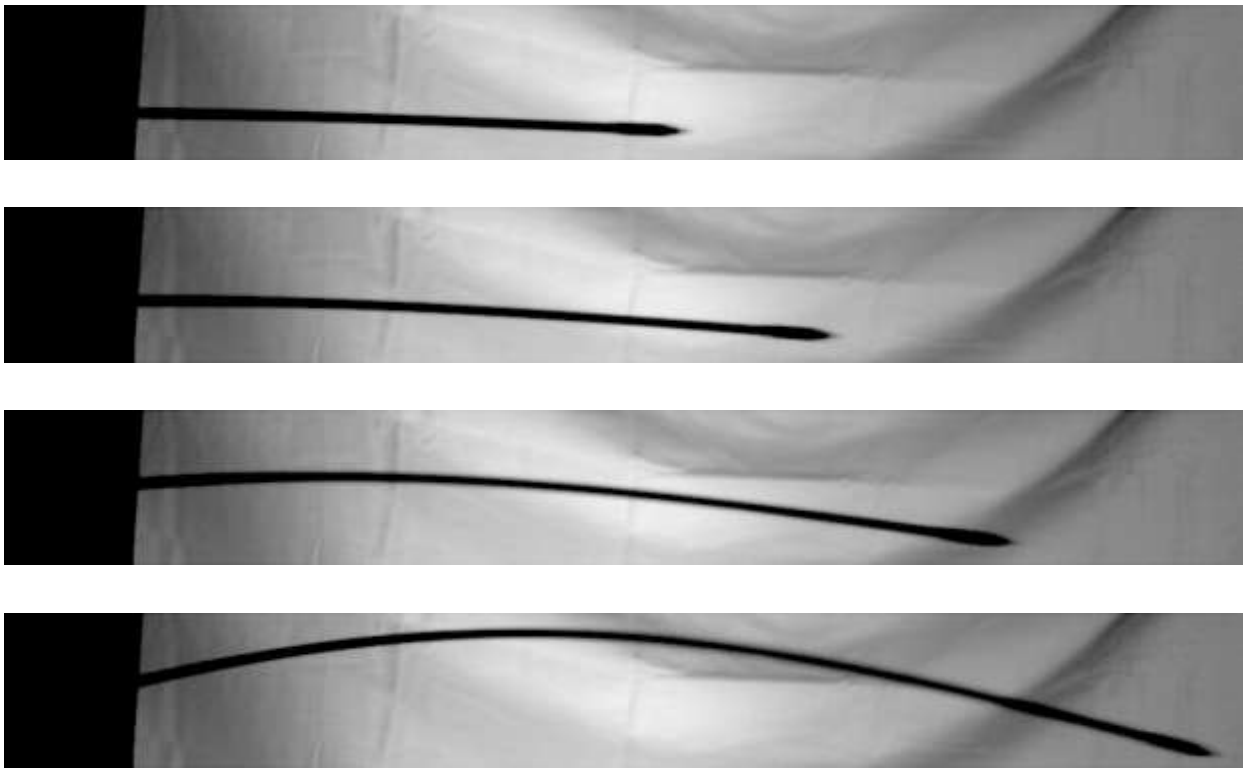

FIG. 8. The extreme buckling of a carbon arrow with a very massive tip, flying from the left to the right.

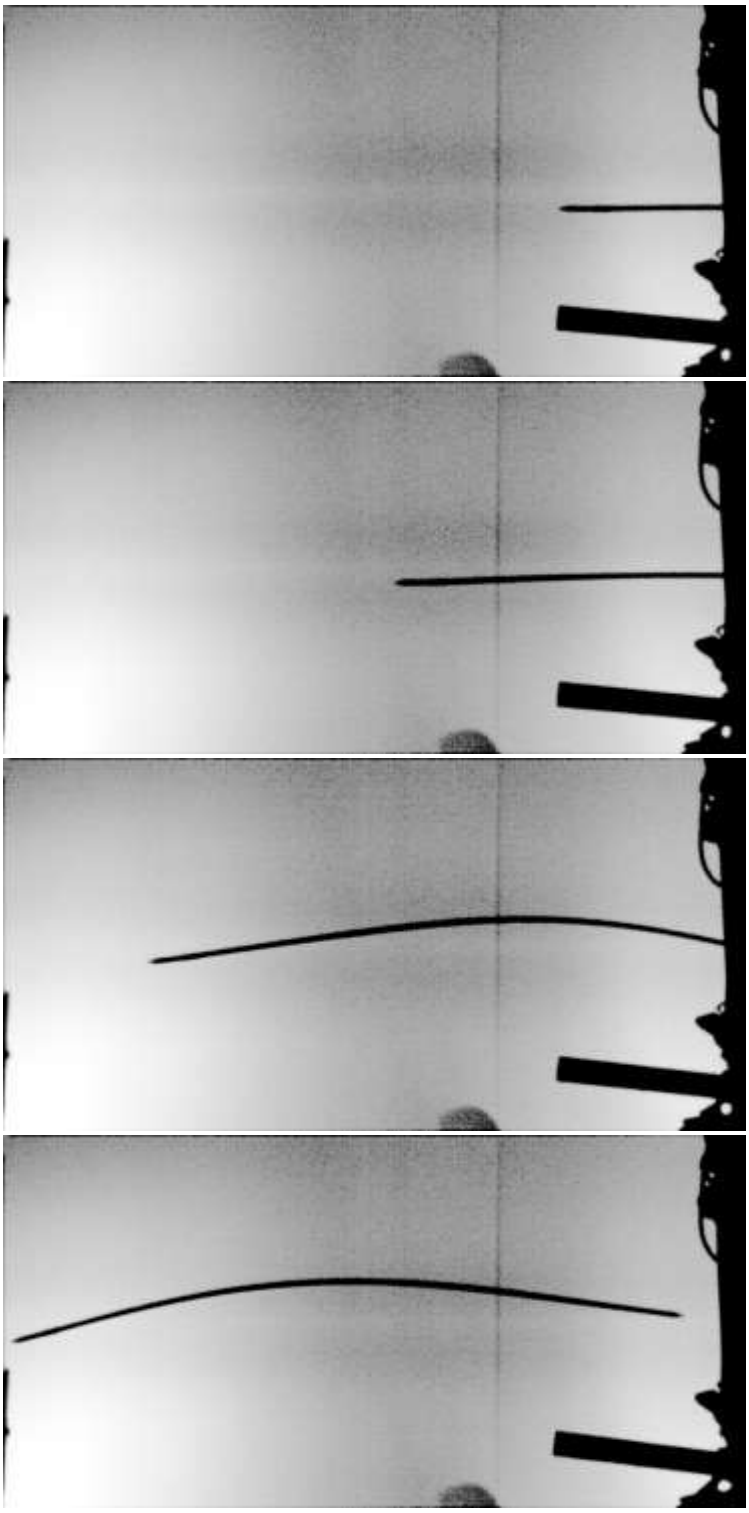

FIG. 9. The buckling of a cedar arrow with a very massive tip.

Chapter 4

Modeling the Buckling of an Arrow

4.1 Methods

A sound strategy for modeling the buckling of any object is to work in the rest frame of the object and consider vibration and rotation about its center of mass. We shall employ such a strategy here to model an arrow in two distinct regimes: as it is accelerated by a bow and as it flies through the air. High speed videos reveal that rotation can be safely ignored, allowing us to focus solely on vibration. Similar to approximations made when modeling the vibration of a string, we consider the vibration to occur solely in a single direction perpendicular to the arrow's flight. We call the direction of vibration the y direction and the direction of flight the x direction, as illustrated in figure 10. The vibration in the y direction is governed by the Euler-Bernoulli equation for the dynamic buckling of a beam [1,5]:

FIG. 10. An arrow of length L in flight, moving in the x direction, will vibrate in the y direction. We use a coordinate system in the rest frame of the arrow with the origin at the nock when the arrow is unbuckled.

$$EI\ \frac{\partial^4 y}{\partial x^4} + \frac{\partial}{\partial x}\left(F(x,t)\frac{\partial y}{\partial x}\right) + \rho A\frac{\partial^2 y}{\partial t^2} = 0$$

Where E is the Young's modulus of the arrow, I is the second moment of inertia of the cross section with respect to the neutral axis of the arrow [2]. The function F(x,t) represents the compression force in the arrow. The constant A is the cross sectional area of the arrow shaft, and ρ represents the density of the arrow, which is taken to be constant. Since a modern arrow is hollow, the following formulae give the cross sectional area and the second moment of inertia [2]:

$$A = \frac{\pi(D^2 - (D-2G)^2)}{4}$$

$$I = \frac{\pi(D^4 - (D-2G)^4)}{64}$$

We examine the two special cases individually. First, we examine the arrow in flight in the inertial rest frame of the arrow, neglecting the compression force present as a result of the acceleration. Then we tackle the problem of an arrow in a non-inertial

reference frame. This requires us to derive the Euler-Bernoulli equation with an additional fictitious force to account for the frame. After deriving the equation, we examine some simple solutions and compare them to the result for an arrow in flight.

4.2 Stress-free Arrow in Flight

Now we will examine the equations of motion governing the buckling of an arrow while it is in flight. To simplify the problem, we neglect the internal stress waves which would be bouncing back and forth inside of the arrow as a result of it being accelerated. In other words, we solve the Euler-Bernoulli equation for a stress free arrow by neglecting the forcing term $\frac{\partial}{\partial x}\left(F(x,t)\frac{\partial y}{\partial x}\right)$. We also treat the arrow as an object of constant density, so we are modeling a tip-less arrow.

First, we establish a coordinate system in the rest frame of the arrow whose origin is at the initial position of the nock when the arrow is perfectly straight, as shown in figure 10. We solve the Euler-Bernoulli equation using separation of variables and Fourier analysis [6].

$$EI\ \frac{\partial^4 y}{\partial x^4} + \rho A \frac{\partial^2 y}{\partial t^2} = 0$$

First, since we are in the rest frame, x and t are independent variables. This allows us to assume a solution of the form:

$$y(x,t) = Y(x)T(t)$$

Plugging this solution into the Euler-Bernoulli equation yields:

$$EI\ \frac{\partial^4 Y}{\partial x^4}T + \rho A Y \frac{\partial^2 T}{\partial t^2} = 0$$

Next we divide by Y(x)T(t) and separate is into two separate equations. Because both sides of the equation involve separate independent variables, they must equal a constant. This yields two ordinary differential equations with four boundary conditions and two initial conditions.

$$EI\ \frac{\partial^4 Y}{\partial x^4}\frac{1}{Y} = -\rho A\frac{\partial^2 T}{\partial t^2}\frac{1}{T} = \sigma$$

$$EI\ \frac{\partial^4 Y}{\partial x^4} - \sigma Y = 0$$

$$\rho A\frac{\partial^2 T}{\partial t^2} + \sigma T = 0$$

We begin by solving the x equation. The characteristic equation tells us that it has a general solution of the form:

$$Y(x) = c_1 e^{\beta x} + c_2 e^{-\beta x} + c_3\cos(\beta x) + c_4\sin(\beta x)$$

$$\beta = \sqrt[4]{\frac{\sigma}{EI}}$$

Next, we apply the four boundary conditions. First we say that the bending moment at the tip and nock vanishes.

$$\frac{\partial^2 y(0,t)}{\partial x^2} = \frac{\partial^2 y(L,t)}{\partial x^2} = 0$$

High videos show the tip of the arrow remains essentially fixed in the y direction, so we treat the arrow like it is on a hinge.

$$y(L,t) = 0$$

Finally, we the establish the condition that the shear force on the nock is zero.

$$\frac{\partial^3 y(0,t)}{\partial x^3} = 0$$

Applying the boundary conditions at x=0 yields the following two conditions:

$$c_3 = c_1 + c_2$$

$$c_4 = c_1 - c_2$$

Applying the boundary conditions at x = L yields the two equations:

$$c_1(e^{\beta L} - cos\beta L - sin\beta L) + c_2\left(e^{-\beta L} - cos\beta L + sin\beta L\right) = 0$$

$$c_1(e^{\beta L} + cos\beta L + sin\beta L) + c_2\left(e^{-\beta L} + cos\beta L - sin\beta L\right) = 0$$

Adding these two equations together allows you to obtain c_2 in terms of c_1. Plugging this back into one of the above equations yields:

$$c_1(cos\beta L\, sinh\beta L - sin\beta L\, cosh\beta L) = 0$$

Letting c_1 equal zero would yield a trivial solution which is of no academic interest. So we want the expression in parentheses to equal zero to obtain a non-trivial solution. Setting this equal to zero yields the following transcendental equation which determines the eigenvalues:

$$tan\beta L = tanh\beta L$$

This equation has infinitely many solutions which determine the value of β, so we rewrite β as β_n. As a result of this, we set $c_1 = 1$ and obtain infinitely many solutions for the x equation.

$$Y_n(x) = c_n(sinh\,\beta_n(x - L) - sinh\beta_n L\, cos\beta_n x + cosh\beta_n L\, sin\beta_n x)$$

Next, we focus on obtaining a solution for the second ordinary differential equation. The characteristic equation tells us that there exists a general solution of the form:

$$T_n(t) = b_1 cos\left(\beta_n{}^2 \sqrt{\frac{EI}{\rho A}}\, t\right) + b_2 sin\left(\beta_n{}^2 \sqrt{\frac{EI}{\rho A}}\, t\right)$$

Combining this with the solution for Y(x) yields the general solution for the entire problem.

$$y(x,t) = \sum_{n=1}^{\infty} [(B_n cos\left(\beta_n{}^2 \sqrt{\frac{EI}{\rho A}}\, t\right) + C_n sin\left(\beta_n{}^2 \sqrt{\frac{EI}{\rho A}}\, t\right))(sinh\, \beta_n(x-L)$$

$$- sinh\beta_n L\, cos\beta_n x + cosh\beta_n L\, sin\beta_n x)]$$

The coefficients B_n and C_n are determined by initial conditions, namely the state of the arrow just as it stops being accelerated by the bow. These initial conditions would be obtained from a full solution to the problem of an accelerated arrow. Specifically, the initial position and initial velocity of the arrow must be known.

$$y(x,0) = Q(x)$$

$$\frac{\partial y(x,0)}{\partial t} = W(x)$$

Using these initial conditions leads us to the following two equations.

$$y(x,0) = Q(x) = \sum_{n=1}^{\infty} [B_n\, (sinh\, \beta_n(x-L) - sinh\beta_n L\, cos\beta_n x + cosh\beta_n L\, sin\beta_n x)]$$

$$\frac{\partial y(x,0)}{\partial t} = \sum_{n=1}^{\infty} [\, C_n \beta_n{}^2 \sqrt{\frac{EI}{\rho A}}\, (sinh\, \beta_n(x-L) - sinh\beta_n L\, cos\beta_n x + cosh\beta_n L\, sin\beta_n x)]$$

If the correct orthogonal function can be found, a Fourier's trick can be used to obtain solutions for the B_n and C_n. At present, we know of no evident solution for this problem, so we leave the correct answer to be determined numerically.

4.3 An Accelerated Arrow

4.3.1 Derivation of the Euler-Bernoulli equation in a Non-Inertial Frame

Modeling the flight of an accelerated arrow using the method outlined in section 4.2 presents one obvious problem: the rest frame of the arrow is non-inertial, since it is being accelerated. This non-inertial frame introduces a fictitious force that may have noticeable effects on the vibration of the arrow. Rather than rethink our strategy of modeling the buckling as vibrations in the object's rest frame, we forge onward by taking into account the effects of the fictitious force on the dynamic buckling of the arrow. This requires us to derive the Euler-Bernoulli dynamic buckling equation by considering the forces acting on a very small differential element of the arrow.

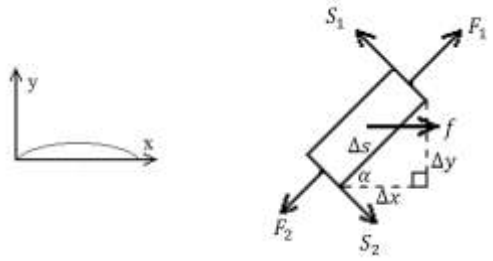

FIG. 11. A schematic depicting the forces acting on a differential element Δs.

First, we consider the arrow as a thin cylindrical rod with a diameter that is small relative to its length. Next, we sum the forces acting on a small, differential element of the arrow along the s direction, as shown in figure 11. Here, F represents the compression force acting on the two circular faces of the element. Note that in this

derivation we define a compression force to be negative. The fictitious force f is a body force, so it acts on the center of mass of the element. The components perpendicular to the arc length s, called S, represent the shearing force that induces a torque on the element. Summing the components acting parallel and perpendicular to Δs yields:

$$F_{s\parallel} = F_1 - F_2 + f cos\alpha$$

$$F_{s\perp} = S_1 - S_2$$

We want to find the resulting motion in the y direction, so we must set the net force in the y direction equal to the acceleration in the y direction:

$$\rho A \Delta s \frac{\partial^2 y}{\partial t^2} = F_{s\parallel} sin\alpha + F_{s\perp} cos\alpha$$

$$\rho A \Delta s \frac{\partial^2 y}{\partial t^2} = (F_1 - F_2 + f cos\alpha) sin\alpha + (S_1 - S_2) cos\alpha$$

Next, we chose to only look at small perturbations in the y direction by invoking a small angle approximation, letting $sin\alpha = tan\alpha$ and $cos\alpha = 1$. At the same time, we point out that this is equivalent to stating that $\Delta s \sim \Delta x$ and take the liberty of replacing all Δs with Δx. Finally, we replace $tan\alpha$ with $\Delta y/\Delta x$ and obtain the following equation:

$$\rho A \Delta x \frac{\partial^2 y}{\partial t^2} = (F_1 - F_2 + f) \frac{\Delta y}{\Delta x} + S_1 - S_2$$

At this point, we remind the reader that F, f and S are all functions of x and t. Rewriting the above equation, we obtain:

$$\rho A \frac{\partial^2 y}{\partial t^2} = \frac{1}{\Delta x}\big(F(x + \Delta x, t) - F(x, t)\big)\frac{\Delta y}{\Delta x} + \frac{1}{\Delta x}(S(x + \Delta x, t) - S(x, t)) + \frac{1}{\Delta x} f(x, t)\frac{\Delta y}{\Delta x}$$

The fictitious force is proportional to both the mass of an individual element and the acceleration of the non-inertial frame, so we can write $f(x, t) = \rho A \Delta x a(t)$. The

function a(t) represents the acceleration of the center of mass in the lab frame. Plugging this result in and taking the limit as Δx approaches 0 gives us the following equation:

$$\rho A \frac{\partial^2 y}{\partial t^2} = \frac{\partial}{\partial x}\left((F(x,t))\frac{\partial y}{\partial x}\right) + \frac{\partial}{\partial x} S(x,t) + \rho A a(t) \frac{\partial y}{\partial x}$$

Finally, we note that the shear force is given by $-\frac{\partial}{\partial x}\left(EI\frac{\partial^2 y}{\partial x^2}\right)$ and obtain the Euler Bernoulli buckling equation for a non-inertial frame:

$$\rho A \frac{\partial^2 y}{\partial t^2} - \frac{\partial}{\partial x}\left((F(x,t))\frac{\partial y}{\partial x}\right) + EI\frac{\partial^4 y}{\partial x^4} - \rho A a(t)\frac{\partial y}{\partial x} = 0$$

4.3.2 Dropping an Arrow

Now that we have derived the relevant equation, we would like to solve it to see how an arrow buckles in a non-inertial frame. So, rather than launch into a full solution of the equation for an arrow, we discuss a much simpler thought experiment: dropping the arrow off of a very tall building. We assume a stress free arrow and the acceleration of the center of mass to be just g, or 9.8 m/s^2. This gives us the equation:

$$\frac{\partial^2 y}{\partial t^2} + \frac{EI}{\rho A}\frac{\partial^4 y}{\partial x^4} - g\frac{\partial y}{\partial x} = 0$$

In this equation x is again the coordinate in the rest frame of the arrow, as shown in figure 10. Since we are in the rest frame of the object, x and t are again independent variables, so we can use separation of variables to turn our partial differential equation into two ordinary differential equations, as in section 4.2. Assuming a solution of the form $y(x,t) = Y(x)T(t)$ yields the two equations.

$$\frac{\partial^2 T}{\partial t^2} + \varphi T = 0$$

$$\frac{EI}{\rho A}\frac{\partial^4 Y}{\partial x^4} - g\frac{\partial Y}{\partial x} - \varphi Y = 0$$

Where φ is an arbitrary constant. These equations have a general solution of the form:

$$T(t) = d_1 cos\sqrt{\varphi}t + d_2 sin\sqrt{\varphi}t$$

$$Y(x) = h_1 e^{r_1 x} + h_2 e^{r_2 x} + h_3 e^{r_3 x} + h_4 e^{r_4 x}$$

Where r_m are the roots to the equation:

$$\frac{EI}{\rho A} r^4 - gr - \varphi = 0$$

This equation possesses no simple analytical solution, but the roots can be obtained numerically using a software package such as Mathematica. We use the same boundary conditions for a free arrow established in section 4.2, namely:

$$y(L,t) = \frac{\partial^2 y(0,t)}{\partial x^2} = \frac{\partial^2 y(L,t)}{\partial x^2} = \frac{\partial^3 y(0,t)}{\partial x^3} = 0$$

We choose to release the arrow in a slightly bent state with no initial velocity in the y direction.

$$y(x,0) = h(x)$$

$$\frac{\partial y(x,0)}{\partial t} = 0$$

At this point, because the roots cannot be obtained analytically, the equation must be solved numerically. Once the roots are obtained, it is not too far of a leap to solve the problem using the same method as in section 4.2. All we can say is that it is curious to note that the fictitious force has a very noticeable impact on the general solution to the

problem. Introducing a fictitious force changes the eigenfunctions needed to describe the vibrations of an arrow drastically.

4.3.3 An Accelerated Arrow

An accelerating arrow can be successfully modeled if the following equation can be solved:

$$\rho A\frac{\partial^2 y}{\partial t^2}-\frac{\partial}{\partial x}\left((F(x,t))\frac{\partial y}{\partial x}\right)+\ EI\frac{\partial^4 y}{\partial x^4}-\rho Aa(t)\frac{\partial y}{\partial x}=0$$

We have experimentally determined a(t) to have the form $a(t)=6(k_n-k_t)t=k_{eff}\,t$. So, plugging this into the equation yields the following:

$$\rho A\frac{\partial^2 y}{\partial t^2}-\frac{\partial}{\partial x}\left((F(x,t))\frac{\partial y}{\partial x}\right)+\ EI\frac{\partial^4 y}{\partial x^4}-\rho Ak_{eff}t\frac{\partial y}{\partial x}=0$$

At present, it is not evident whether analytical solutions exist to this equation. The addition of the fictitious force term makes the equation un-seperable, meaning that standard Fourier analysis is obsolete. Laplace transformations also fail to simplify the problem because of the same term. The best that one can currently do is resort to numerical solutions of the equation.

Chapter 5

Conclusion

Archery opens the door to exciting new regimes of buckling which require a rich tapestry of physics and mathematics to properly describe. This thesis has merely attempted to lay the foundations for further study of the dynamic buckling of arrows in flight. First, we observed the phenomena experimentally by constructing a precise shooting machine and imaging it with high speed cameras. We developed methods for measuring the compression force and fictitious force acting on the arrow. We derived the Euler-Bernoulli equation for a non-inertial frame, and found that it obtains drastically different eigenfunctions than equivalent solutions in an inertial frame. Ultimately, we discovered that the non-inertial forces must be taken into account to accurately model the acceleration of an arrow.

References

[1] R. Pekalski, Journal of Sports Sciences **8**, 259 (1990)
[2] B. W. Kooi, et al, Journal of Sports Sciences **16**, 721 (1998)
[3] B. W. Kooi, Journal of Engineering Mathematics **31**, 285 (1997)
[4] B. W. Kooi, History of Technology **20**, 125 (1998)
[5] J. R. Gladden, et al, Phys. Rev. Letters **94**, 035503 (2005)
[6] E. Kreyzig, *Advanced Engineering Mathematics* (Wiley, New Jersey 2006) p. 540

Curriculum Vitae

Education:
The Pennsylvania State University, University Park, PA
B.S. in Physics with Honors, Expected May 2010
Minor in Mathematics, Expected May 2010

Thesis:
"Dynamic buckling of free rods in flight"
Thesis advisor: Andrew L. Belmonte (Dept. of Mathematics)

Funding:
NSF Graduate Research Fellowship — *April 2010*

Publications:
- Steven J. Full, J. P. McNutt, Milton W. Cole, et al, "Anomalous effective dimensionality of quantum gas adsorption near nanopores", Journal of Physics: Condensed Matter. (Submitted) — *Dec. 2009*
- J.B. Rosenzweig, G. Andonian, P. Bucksbaum, M. Ferrario, S.J. Full, et al, "Teravolt-per-meter plasma wakefields from low-charge, femtosecond electron beams", Physical Review Letters. (Submitted) — *Nov. 2009*

Research Experience:

Beam and Accelerator Physics at UCLA — *June – August 2009*
- Studied the creation of teravolt-per-meter electric field gradients in a plasma wakefield accelerator
- Modeled the accelerator design using particle-in-cell simulations
- Presented work in an undergraduate symposium at UCLA — *Sept. 2008 – Sept. 2009*

Surface Physics at Penn State
- Theoretically explored gas adsorption in carbon nanotube systems
- Discovered anomalous dimensionality in diverging tube geometry
- Gained fluency in Mathematica and computational methods

Teaching Experience:

Tutor for Penn State's Multicultural Engineering Program — *2008-2009*
- Tutored introductory level Physics courses to engineering, science, and pre-medicine majors

Physics and Mathematics Specialist for the Penn State Educational Partnership Program — *2006-2008*
- Taught physics and geometry to a classroom of high school students in an after school program
- Mentored disadvantaged youth and motivated them to pursue a college education

Volunteer Tutor for the Society of Physics Students — *2009-2010*
- Aided students in mastering the material for both introductory and advanced Physics courses

Honors:
The Evan Pugh Scholar Award (Junior and Senior)

The President Sparks Award
The President's Freshmen Award
Penn State Faculty Award for Academic Excellence in Science

Affiliations: Schreyer Honors Scholar
Sigma Pi Sigma Member